Insect monitoring with fluorescence lidar techniques: field experiments

Zuguang Guan,[1,*] Mikkel Brydegaard,[1] Patrik Lundin,[1] Maren Wellenreuther,[2] Anna Runemark,[2] Erik I. Svensson,[2] and Sune Svanberg[1]

[1]Atomic Physics Division, Lund University, P.O. Box 118, SE-221 00 Lund, Sweden

[2]Department of Biology, Lund University, SE-223 62 Lund, Sweden

*Corresponding author: zuguang.guan@fysik.lth.se

Results from field experiments using a fluorescence lidar system to monitor movements of insects are reported. Measurements over a river surface were made at distances between 100 and 300 m, detecting, in particular, damselflies entering the 355 nm pulsed laser beam. The lidar system recorded the depolarized elastic backscattering and two broad bands of laser-induced fluorescence, with the separation wavelength at 500 nm. Captured species, dusted with characteristic fluorescent dye powders, could be followed spatially and temporally after release. Implications for ecological research are discussed. © 2010 Optical Society of America

OCIS codes: 280.3640, 300.2530.

1. Introduction

Lidar techniques have been developed for almost 50 years for atmospheric monitoring by analyzing the return echo from the aerosols distributed in the atmosphere [1–3]. The fluorescence lidar variety is useful in assessing phenomena in addition to those relying on elastic backscattering from aerosols. Because of the existence of alkali atoms and iron ions in an extremely low-pressure environment, fluorescence lidar is a unique technique for monitoring conditions in the upper atmosphere [3]. At a shorter range, the Swedish research group at Lund University, and others, have shown that remote targets within a few hundred meters can be analyzed successfully using laser-induced-fluorescence (LIF) spectroscopy [4]. Based on a well-developed mobile lidar system [5], the applications range from the optical diagnosis of historical monuments to the analysis of hydrological and vegetation targets. With the knowledge of measurements ranging from aerosols with sizes of less than 1 μm to macro solid targets, such as the Roman Colosseum [6], we are currently at the intermediate spatial scale by studying flying insects.

Monitoring insects and studying their movements is of great importance in biological research and environmental monitoring. For instance, damselfly larvae are highly sensitive to water pollution and dissolved oxygen concentrations and, thus, are used as biomarkers [7]. Like other ectotherms, damselflies are sensitive to ambient temperature, and many species have undergone a northward shift in their distribution due to global warming [8]. Dispersal studies of insects are also critical for understanding the role of dispersal between populations over wide spatial scales [9], which is important when developing conservation policies. The traditional method is limited to marking individuals with different dyes and then collecting individuals from neighboring populations [10]. Advanced remote detection techniques in this field have developed slowly. Pioneering work using elastic lidar to study honeybees for land mine detection has been reported [11–13].

Noticing the potential advances of LIF techniques in insect monitoring and the natural connection with the dye markers used for traditional tracing, we

demonstrated for what is believed to be the first time fluorescence lidar techniques for damselfly (*Calopteryx splendens* and *C. virgo*) monitoring at a distance of 60 m [14]. For initial remote spectral analysis of LIF, an intensified fiber-coupled optical multiple channel analyzer system [15] is employed. By averaging signals, even the autofluorescence from mounted dead damselflies was useful for distinguishing between species and sexes [14]. Importantly, damselflies dusted with different types of dye can be spatially resolved and distinguished from the fluorescence signature in a single lidar pulse. To further test the feasibility of such a technique, two weeks of field experiments were carried out in southern Sweden, where three geometrical arrangements were set up over a river surface [see Fig. 1(a)], and damselflies that were flying into the laser beam were detected and counted statistically. During the campaign, three groups of damselflies were dusted with dye powder and released into the natural environment. The fluorescence signatures in lidar signals reveal their presence, dispersal patterns, and activity in later measurements.

This paper is organized as follows. First, the fluorescence lidar equipment is introduced in Subsection 2.A, followed by a description, in Subsection 2.B, of the geographic setting of the field experiment where three lidar paths are set up. The selection and use of fluorescence dyes in the short-range test and in the field experiments are described in Subsection 2.C. Subsection 3.A shows a method used to distinguish three species of damselflies (dusted with different dyes) using their fluorescence signatures. In Subsection 3.B, the statistical results are presented and discussed in the spatial domain, as well as in the time domain, also taking weather conditions into account. In addition, the application of a method used to extract insect echoes out from the electronic perturbance is introduced in Subsection 3.C. Finally, we discuss the general applicability of the technique in biological systems and the biological implications of the findings.

2. Experimental Methods

A. Lidar Equipment

The experimental facility is based on the Lund mobile lidar system [5], which is modified for the current study in important ways. The main equipment is presented in Fig. 1(b). The third harmonic (355 nm) of the Nd:YAG laser radiation is used with an energy of 40 mJ/pulse, and with a pulse width of 10 ns. After expanding to a beam diameter of 5 cm, the laser beam is transmitted by a mirror (40 cm × 56 cm) placed in a transmission dome, which can scan vertically and horizontally. A quartz window in the dome is used to protect the mirror from atmospheric dirt and dust. The elastic scattering and the fluorescence from the targets are reflected by the same mirror and collected by a telescope system with a diameter of 40 cm. The collected light is distributed by several mirrors and is filtered, and then detected by three photomultipliers (PMTs). As shown in Fig. 1(b), the elastic scattering from the target is selected by a laser line mirror (LM) and recorded by PMT-1 in the time domain. A polarizer (P) is set at a crossed angle against the polarization state of the transmitted laser beam. Therefore, PMT-1 is sensitive only to depolarized backscattering, but blind to the copolarized echo from the target surface, and, hence, insensitive to the flying orientation of the insect in the laser beam. An extra-short-pass filter (SF) is used to suppress the fluorescence light from the target and background light from the sky thereafter. The fluorescence light passing
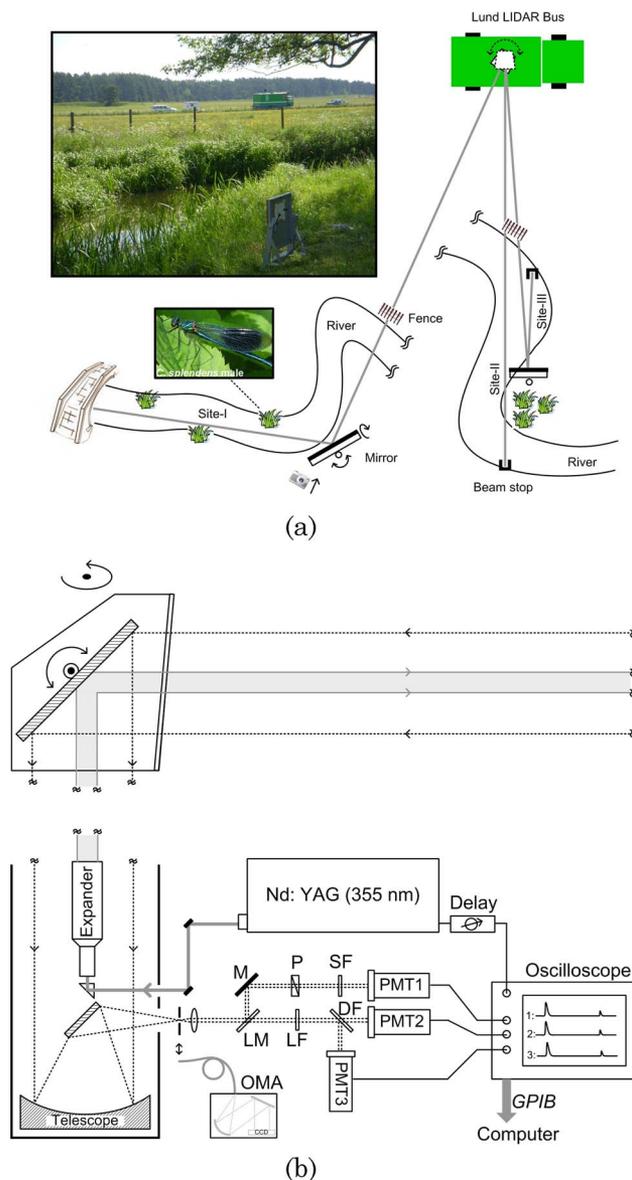

Fig. 1. (Color online) (a) Geographic diagram of the measurement locations. The inserted scenery picture is taken from the indicated position and direction; also shown is a male *C. splendens* damselfly. (b) Key equipment/components of the fluorescence lidar (PMT-1 is for detection of elastic scattering, while PMT-2 and PMT-3 are for yellow and blue bands of fluorescence, respectively).

through the LM is divided by a dichroic filter (DF) into two wavelength bands, blue (400–500 nm) and yellow (500–750 nm), and measured by PMT-3 and PMT-2, respectively. Before the DF, a long-pass filter (LF) is used to suppress the leakage of the elastic scattering through the LM. Three channels of signals from the PMTs are simultaneously recorded by a high-speed oscilloscope (Tektronix TDS544B), which samples every 8 ns. The start time of the sampling period is controllable by adding a tunable delay onto the synchronization trigger from the Nd:YAG laser. The recorded data are then read out through a GPIB connection by a computer in real time. The repetition rate of the whole system is limited to 10 Hz by communication speed, although the repetition rate of the laser system is 20 Hz. By using such a three-PMT system, both the elastic scattering and two bands of fluorescence can be analyzed in the time/spatial domain.

B. Field Site

Insect measurements were performed with the Lund mobile lidar system at the Klingavälsån river, Veberöd (55°38′ N, 13°29′ E), in southern Sweden, during two weeks (1–7 and 24–30 June 2009); see Fig. 1(a). The vehicle was parked near the river, and the laser beam passed over a pasture enclosure, and was measuring in three different geometrical arrangements over the surface of the river. In the first week, the measurements were carried out at Site I, where the laser beam was folded by a plane mirror (∼50 cm × 60 cm) in order to be close to the water surface, and then terminated below a bridge. The insects flying through the laser beam could be measured and analyzed in real time. In the second measurement week, the laser beam was moved to Sites II and III. At Site II, the laser beam followed a section of the river that included a peninsula and the beam was terminated by a black beam stop that was set up at the riverbank. Close to Site II, Site III was set up by folding the laser beam closer to the river surface, using the same plane mirror, but now mounted on the peninsula.

Single-pulse lidar echoes corresponding to three paths of the laser beam are shown in Fig. 2, correlated to a satellite image (obtained via the Google Earth tool) of the field. The backscattered signals from the static targets, including the quartz window (protecting the rooftop lidar mirror), a fence, the folding mirror, and the termination, are shown to be stable in all three bands during the long-term measurements. Ranges of interest are marked out in Fig. 2(a) and corresponding lidar echo signals are shown in Fig. 2(b). For instance, in Path I, the range between the mirror and the bridge, corresponding to Site I [compare with Fig. 1(a)], is from 186 to 260 m. Any small "blips" in between the fixed target echoes that show up in the elastic band are recorded by the system, and later counted as one detection in the histogram. The two fluorescence bands are basically used for analyzing dusted-and-released damselflies

in the second measurement week, since the auto-fluorescence from natural damselflies was too weak to be measured in a single pulse in daylight conditions, while the dye-induced fluorescence can easily be distinguished. From the static targets, we can see fluorescence signatures from the quartz window (due to the dust and dirt attached on the surface), but not (or very weakly) from the metal fence, while they saturate the PMTs at the black-painted terminations. We realized that the intensity of the fluorescence signal from the quartz window can be used for normalization, so that the instabilities of the fluorescence
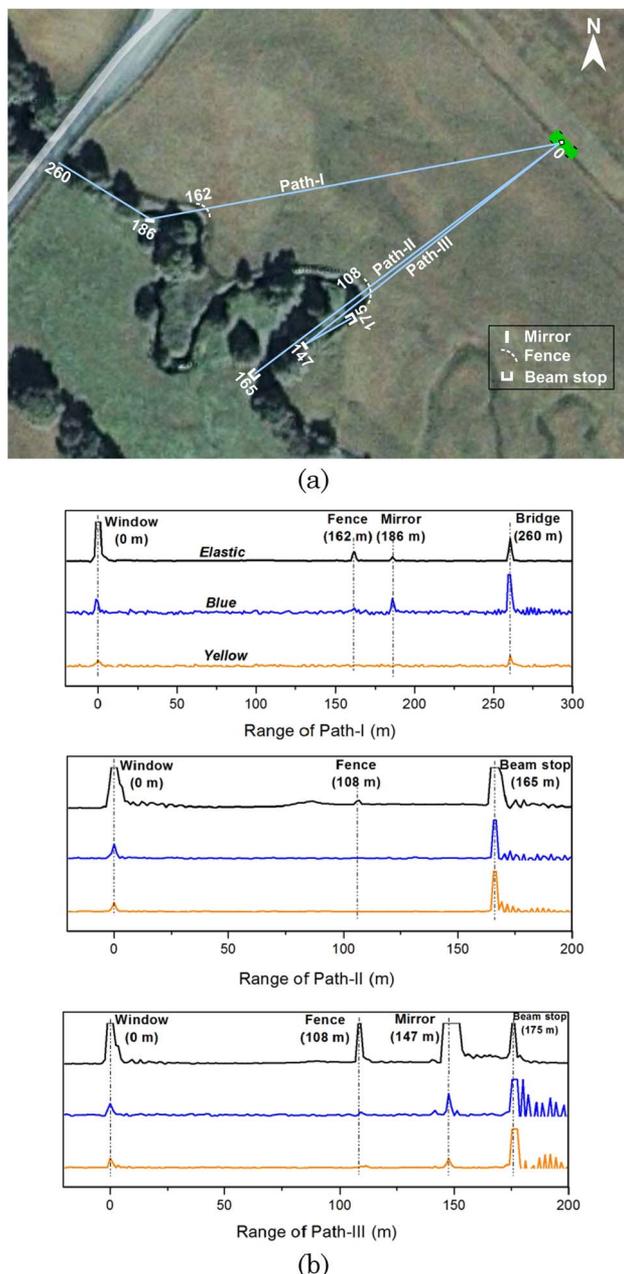

(a)

(b)

Fig. 2. (Color online) (a) Three lidar paths are shown on a satellite map; numbers indicate the lidar–target distances in meters; (b) lidar echoes from the static targets in Path I (top), Path II (middle), and Path III (bottom).

signals, depending on the laser power, PMT sensitivity, etc., can be compensated for.

C. Application of Dyes

Before the field experiments, the performance of the lidar system was tested in Lund. Two dead *Calopterygiid* damselflies marked with different dyes (Coumarin 102 and Rhodamine 6G) were placed at different distances (60 and 80 m, respectively) within the laser path; see Fig. 3(a). The single-pulse reflection signal burst from the damselflies was then recorded by the three-PMT systems, as shown in Fig. 3(b). Obviously, the intensity (ratio) of the two fluorescence bands are different for the damselfly positioned at a closer distance, which is marked by Coumarin 102, a bluish dye, and the other one at a larger distance, marked by Rhodamine 6G, which is reddish. The fluorescence spectra of these two dyes for 355 nm excitation are shown in Fig. 10 of Ref. [14]. The above tests indicate that the fluorescence signature from a single lidar pulse is sufficient to distinguish damselflies marked with different dyes, which was encouraging for studying flying damselflies in their natural habitats.

In the later field experiments, three types of dye powder from Swada Inc. were used to dust three groups of captured damselflies belonging to the species *C. splendens* and *C. virgo*. Specifically, 43 *C. splendens* males were marked with Stellar green, 19 *C. splendens* females were marked with Comet blue, and 20 *C. virgo* males were marked with Nova red. It is worth mentioning that these dye powders are used regularly by biologists for dispersal and mating studies (see, e.g., [10]), and have been tested to not harm the insects. The fluorescence spectra for 355 nm excitation are shown in Fig. 4. With the cutoff wavelength of the dichroic filter, which distributes the light energy into two PMTs, at 500 nm, one can expect that the blue dye will mainly be seen by the
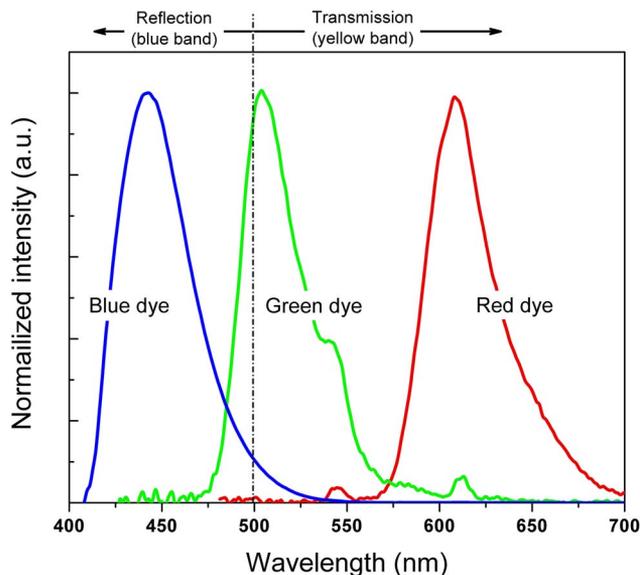
Fig. 4. (Color online) Fluorescence spectra of three dye powders used in the field experiments, with excitation wavelength at 355 nm. The dashed–dotted line indicates the cutoff wavelength of the dicroic filter.

blue-band PMT, while the red dye will be seen by the yellow-band PMT, and the green dye by both. Dusted damselflies were released at Site III during the measurement in the second week, 29 and 30 June 2009. They appear occasionally in the laser path together with unmarked damselflies, and are distinguished by the lidar system from them by the fluorescence signatures. Since the different species and sexes are dusted with different powders, information on species- and sex-specific habitat preferences and dispersal patterns can be obtained if a large enough number of insects is dusted and released. For calibrating the signals at the two fluorescence bands, glass tubes with the individual dyes are moved in and out of the laser beam (close to the fence) to get the standard fluorescence signatures. A detailed analysis of this procedure is given in Section 3.

3. Data Analysis

A. Fluorescence Signature

The method of the fluorescence analysis of damselflies is described here. Figure 5(a) shows several examples of single-pulse lidar curves corresponding to different situations/events happening at Site III. The background consists of static signals (in the situation of no damselfly), and obvious "blips" (with the underlying area filled in) can be occasionally seen between the fence and the mirror (marked by light yellow shaded band), when damselflies fly into the laser beam. For the unmarked damselflies, the signals in the two fluorescence bands are not obvious due to the weak autofluorescence; however, the elastic backscattering is enough for statistical counting (see Subsection 3.B). For the dusted-and-released ones, the fluorescence signatures are clearly different for the three dye species. As expected, the blue
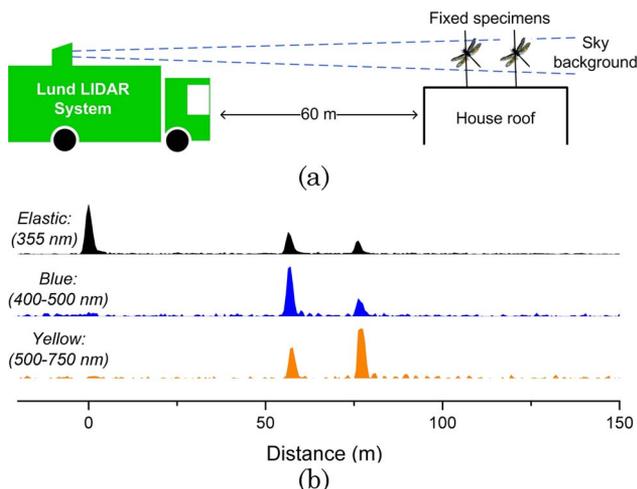

Fig. 3. (Color online) (a) Setup for the test-range measurements, and (b) range-resolved signals of the three channels, from two serially placed damselflies marked with different dyes (Coumarin 102 and Rhodamine 6G).

dye shows a stronger bluish fluorescence, while the red dye shows stronger fluorescence in the yellow band, and the green one shows a relatively equal intensity in both bands.

The echo signals corresponding to the damselflies observed in the two fluorescence bands are normalized to those arising from the quartz window at distance 0, before they are plotted in the scatter plot in Fig. 5(b). Here the echo energy is calculated by integrating the echo return intensity in the time domain. By doing so we obtain higher accuracy than by simply selecting the peak intensity, considering that the laser pulse width (10 ns) is comparable with the sampling temporal interval (8 ns). As mentioned above, the dye tubes were used for calibration. The normalized signals corresponding to these "standard" samples are first plotted in Fig. 5(b) as crossed marks, which separate clearly. The blue and red dyes occupy the upper-left and bottom-right areas, respectively, due to relatively strong bluish and yellowish fluorescence, while the green dye signals, with equal intensities in both bands, are situated in between. With such a calibration method, the signals corresponding to the dusted damselflies can be plotted into the same scatter plot and their respective dyes can be determined based on which area they are located in. The data from the field measurement of flying dusted-and-released damselflies are shown as round marks in the figure, and the three groups are well distinguished.

B. Statistical Analysis

Using the strategy described in Subsection 3.A, damselflies that appear in the laser beam were detected and statistically counted. The range-resolved results are shown in Fig. 6. For Site I, the data close to the mirror are disturbed by the riverbank vegetation moving in the wind. Many of the measured insects that were found close to the bridge were mosquitoes (according to visual observations), which cause weaker echoes than the damselflies. Mosquitoes and damselflies can thus be separated by adjusting the threshold for selecting echoes. The decay of the lidar curve with range (R), following R^{-2}, has been considered when setting the threshold. Damselflies were mainly detected between 210 and 250 m. Three signal locations, indicating positions in which damselflies frequently appeared, were correlated with reed stands (preferred territories of damselflies [16]). For Site II, damselflies were mostly found around the peninsula, which was consistent with our visual observations. It is interesting to compare the results with Site III, where the peninsula was occupied by the mirror. During the measurements at Site III, we released three groups of damselflies near the fence on 29 and 30 June 2009. In later measurements, they are recorded, distinguished, and plotted in Fig. 6(c). The spatial distribution of the marked damselflies is comparable with that of the unmarked individuals.

Statistical analyses were also performed in the time domain. Figure 7 shows the result obtained at Site I, on 2 June 2009, together with the weather parameters. The damselflies were identified (shown in black) using the threshold method described above. The number of actively flying insects (including both mosquitoes and damselflies) decreased considerably as the temperature dropped and wind speed increased. The observed increase of damselflies in activity between 15:00 and 16:00 is probably
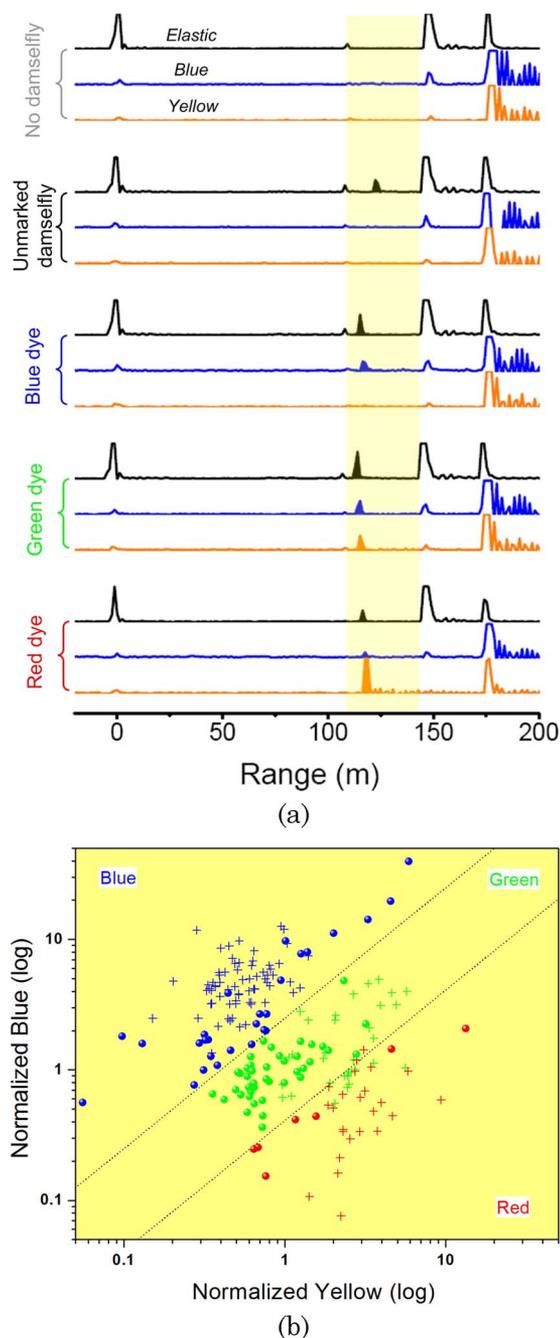

Fig. 5. (Color online) (a) Lidar signals showing different events at Site III, and (b) the scatter plot showing the fluorescence properties of three types of dyes; the crosses and the round marks indicate the calibrating dye tubes and the dusted damselflies, respectively.
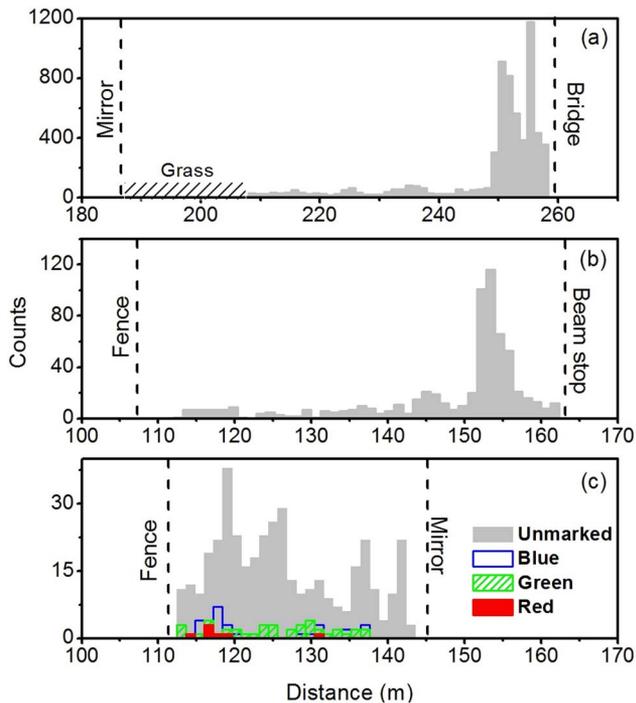
Fig. 6. (Color online) Spatial distributions of the flying damselflies at (a) Site I, (b) Site II, and (c) Site III. The colored histograms in (c) indicate dusted-and-released damselflies. The females marked with blue dye and males marked with green dye belong to the species *C. splendens*, whereas the males marked with red dye are *C. virgo*.

due to other environmental factors, such as increased Sun radiation due to local cloud movements. Results from the three consecutive measurement days at Site III, where dusted damselflies were released on 29 and 30 June 2009, are shown in Fig. 8. From the figure, it can be seen that several of the marked damselflies were alive on 30 June 30 2009, which corresponds to 1–2 days after they were originally marked.

C. Perturbation Removal for Enhanced Damselfly Detection

One particular feature of insects in lidar data is their sudden temporal occurrence and disappearance, which is in great contrast to influences of perturbing static objects along the line of propagation of the light pulse. Such completely static features could, in principle, have been removed simply by subtracting an "empty" curve that contains only static information [such as the curves shown in Fig. 2(b)] from all measurements. In the real world, the strong reflections from the fence and the mirror in this case, can induce nonoptical features, e.g., oscillations caused by electronic reflections in the PMT cables or depletion of the charges in the dynodes. Such an unstable perturbance, together with a triggering uncertainty from the quasi-static features in the backscattering signal, makes the simple subtraction approach inapplicable, especially in the range closely after the mirror [see Fig. 5(a) from Site III], where the insect signals can be easily masked. Therefore, we investigated
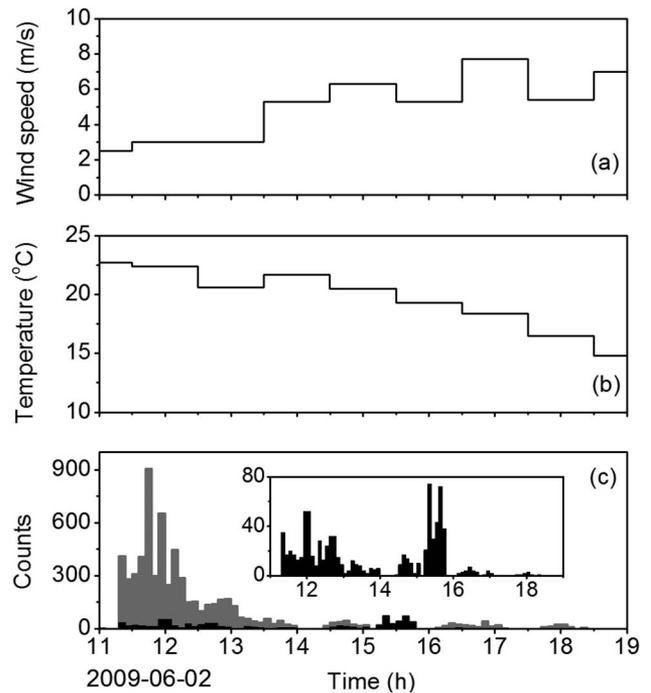

Fig. 7. (c) Measured counts of all insects (gray) and damselflies only (black) activity correlated to (a) the wind speed and (b) the temperature, at Site I. The inset of (c) shows the details of the histogram corresponding to damselflies.

the possibility of removing these quasi-static effects from the data by using the singular value decomposition (SVD) method [17]. SVD is generally not considered suitable for describing temporal phenomena; however, it can be applicable in some cases as a quick tool that requires no detailed information, as traditional input–output system identification methods would [18,19]. We successfully managed to describe the quasi-static background as a linear combination of three time series generated with SVD. As the insects only occur in about one out of a thousand shots, these events will be heavily suppressed by the data not involving a hit. The result of the removal can be seen in the example in Figs. 9(a) and 9(b). In this case, the insect echo is completely hidden in the ringing of the elastic PMT after the strong diffuse reflectance from the mirror [Fig. 9(a)]. While single pulses in any of the PMTs might be caused by "ghost photons" with intensity levels above the background,
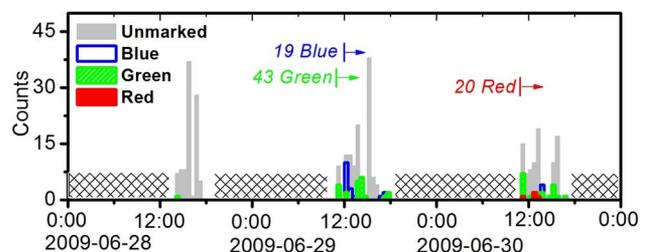

Fig. 8. (Color online) Three days of measurements at Site III. Gray and colored histograms indicate unmarked and dusted damselflies, respectively. Times for release of the dusted damselflies are marked. No measurements are performed during the periods marked by cross-hatching.
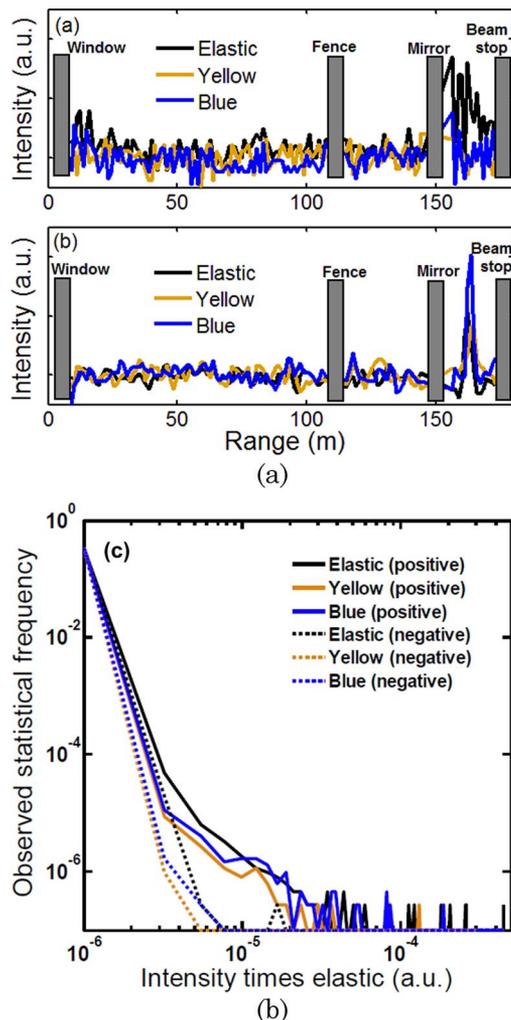
Fig. 9. (Color online) (a) Typical raw echo return after subtraction of "empty" curves (see the text). (b) Signal from the same shot after removing the quasi-static contribution from electronic oscillations, etc. The hit was detected on 29 June 2009, 11:35:27. (c) The insects give rise to a skewness in the intensity histogram. The dotted curves are the negative values. The separation indicates that the insects do, in fact, give an increased intensity return.

it is much less likely that such pulses occur simultaneously in two of the PMTs. One way to increase the contrast of true hits in respect to the ghost photons is to make use of the fuzzy logical AND operator, namely, to multiply the fluorescence signal by the elastic signal. This method is especially valid for marked damselflies that show obvious signals in fluorescence bands. After the removal of the quasi-static contribution, unbiased histograms can be produced on the returned fluorescent intensities times the elastic. In Fig. 9(c), we have produced such a histogram for the range between the fence and the mirror at Site III. The statistics are carried out on three time sections of totally 3 h on 29 and 30 June 2009. To study the insects in particular, the data containing information of road dust plumes from passing cars (discussed below) were excluded. The negative values generally represent the noise level; their amplitudes are plotted with dotted curves to compare with the

positive values plotted as solid curves. Clearly, the reflection signals from the insects produce much higher positive values compared with noise and, hence, induce a skewness in the histogram; see the mismatch between histograms in Fig. 9(c) corresponding to positive and negative values. Similar graphs were observed from the window to fence and the mirror to the termination stretch, although with less and more skewness, respectively. This is in accordance with the ecological *a priori* knowledge, with lower damselfly numbers at the closer range where the laser beam passes the pasture field, but a higher possibility of capturing the flying damselflies over the river surface at the farther range. The SVD method discussed above for quasi-static signature removal works consistently, and was applied successfully over several days of measurements. Figure 10 shows an example in which the removal method works on 25 s of data recorded in the afternoon of 29 July 2009. The three (elastic, blue, and yellow) bands of signals, with quasi-static features removed, are plotted as blue, green, and red, respectively, into a RGB false color map. All three channels are multiplied by the elastic channel to further enhance the contrast. Before the fence, a road dust plume induced by a passing car can be clearly seen on a zero background, thanks to the successful removal of the static/quasi-static features. Particularly, in the range between the mirror and the termination, where originally the insect echo was impossible to see before the removal operation, now clear information appears in different false colors due to different fluorescence performance. The green-dyed damselfly, with reflection signals in all three channels, shows as white in the map, while the natural (nondyed) one
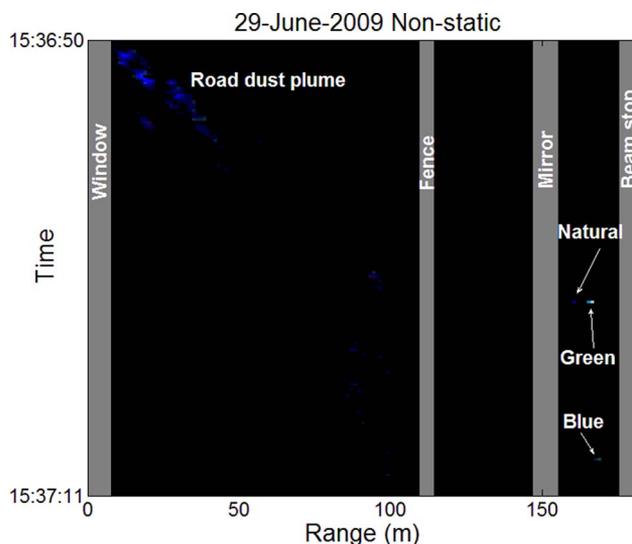

Fig. 10. (Color online) False color RGB representation of 25 s of lidar data with the quasi-static signal removed. Blue, elastic; green, blue fluorescence; red, yellow fluorescence. The inorganic road dust from a passing car gives rise to distributed elastic scattering signals, moving in the wind. The insect signatures appear only for a fraction of a second.

shows up as blue and the blue-dyed one shows up as cyan.

4. Discussion

In this paper, we demonstrate the potential of lidar as a remote-sensing technique to model the spatial and temporal activity of *Calopteryx splendens* and *C. virgo* damselflies in the wild. Although several review articles on the potential of lidar in habitat modeling have appeared in the last few years, the number of applications on natural populations is low, and most of the studies until now have concentrated on bird habitats [20,21] rather than on birds themselves. In particular, we show that lidar can be applied to monitor unmarked damselflies in their natural habitats, and how the use of fluorescent dust helps to differentiate between damselfly sexes and species using a single lidar pulse. Applying such a computerized imaging setup on scales ranging from 100 m to a couple of kilometers will enable biologists to design new experiments and to address new and interesting questions regarding insect ecology, evolution, or optimal wing morphology. In addition, lidar monitoring is an efficient way to assess, for example, population sizes, lifetimes, and dispersal distances and rates, and such data are commonly needed for conservation planning.

Studying the ecological requirements and habitat use of invertebrates in a quantitative way is usually both time consuming and difficult. By using lidar, we show that quantitative data on the temperature and wind speed requirements of *C. splendens* and *C. virgo* can easily be collected during only a few days in the field. For ectotherms, like these damselflies, data on thermal tolerance ranges will be increasingly important in the face of global warming [22,23], since it might tell us about the prospects for local extinction or predict potential northward shifts in the distribution of species. In addition, we have estimated the type of vegetation and at which distances from the water the two species of damselflies occurred, and this adds additional important information about the environmental requirements of these species. Furthermore, the stationary nature of lidar allows the rapid assessment of temporal and spatial activities of individuals in a population. Data collection in such a setting would also be more objective, compared to commonly employed visual censuses by humans, which would increase comparability between sites and observers. Through the marking of different species and sexes with different types of fluorescent dyes, we could also estimate the dispersal patterns and rates of the marked damselflies, and study if habitat use is sex or species specific. This approach would also be useful for mark–recapture studies, a common technique for estimating population sizes where the recapture rate is usually the limiting factor.

From Fig. 6, a tendency for male *C. splendens* (marked by green powder) to be more dispersed along the river than *C. splendens* females and *C. virgo* males can be seen. The difference in dispersion between males of the two species can be attributed to two factors. First, *C. virgo* males have been shown to be more aggressive than *C. splendens* males and are, thus, more dominant [24–26]. This difference in competitive ability is likely to result in the displacement of some *C. splendens* males from their preferred territories, and interspecific contests between males will also often lead to males of *C. splendens* being chased away by *C. virgo* males. Hence, *C. splendens* males might more often be actively displaced from their river territories than males of *C. virgo* and, hence, be in search for new territories. Second, male *C. splendens* commonly force copulations with females, while *C. virgo* males are more likely to perform a courtship display to initiate mating [27]. Forced copulations are being achieved by following flying females and then by forcing the females to bring up their abdomen to engage genitalia [28]. The chasing of females probably contributes to the wide dispersion of *C. splendens* males, thus further increasing the overall spread of males along a river. It should be noted from our result that *C. splendens* males were more dispersed along the river than females, contradicting previous findings, but this might be an artifact of the scale of different studies. A tendency for females to disperse greater distances than males has been observed in both *C. splendens* [29] and in the blue-tailed damselfly *Ischnura elegans* [30]. However, our study measured fine-scale dispersion patterns (scale of a few meters), while the two aforementioned studies investigated large-scale dispersion patterns (hundreds of meters), which were not measured in the current study. Thus, it is possible that the different results are caused by different scales at which the studies were conducted, and that small and large dispersion patterns differ between the sexes of *C. splendens*. In order to address this explicitly, more studies are needed to rigorously test this prediction. The finding that males prefer vegetated habitat near the water is consistent with previous studies on habitat use in these species [26,31]. Aquatic plants provide *C. splendens* males with good perching spots, and oviposition territory for females [32].

Biodiversity is diminishing at an accelerating pace [33], and, therefore, data on biodiversity and spatial distribution are urgently needed for conservation planning. However, the lack of taxonomists and funds precludes particularly the mapping of taxonomically diverse groups, such as invertebrates [21]. Therefore, management strategies mostly concentrate on charismatic vertebrates and only a few conspicuous invertebrates and ignore most other species [34]. However, the diversity of invertebrates is declining even more rapidly than that of plants and vertebrates [35], even though invertebrates are involved in important ecosystem functions, such as pollination and food webs. We thus clearly need better methods to rapidly, effectively, and cheaply assess the abundance and distribution of invertebrate species. The

results of our study are, therefore, encouraging and timely for future assessments of invertebrates.

5. Conclusions

Following proof-of-principle measurements [14], we have now performed successful real-world field experiments on insects *in vivo* and demonstrated the potential of the technique. Lidar provides simple but ecologically meaningful variables for a rapid extrapolation of activity, richness, and composition of insect assemblages across large areas. This enables conservationists to evaluate habitat over large areas and to define diversity hot spots, as well as to monitor changes in the distribution and abundance in response to environmental change. Low fluorescence yield of chitin at 355 nm excitation is a limitation when using nondyed species. However, improvement could be expected by employing, e.g., 266 nm (quadrupled Nd:YAG laser), or 308 nm (XeCl excimer laser) for a better match to the chitin absorption band. Further, the extended fluorescence band available then would also enhance the chance for classification without marking. We did not note any perturbance of the measured species when hit by 355 nm light; however, a shorter excitation wavelength would also be desirable to decrease such a possibility. Full sunlight measurement conditions were shown to be possible; clearly performance is improved for lower light levels. The fact that we estimate a probability rather than a concentration as in, e.g., aerosol lidar applications, implies that a large number of laser shots, in our case thousands of shots, are required to produce a good statistical distribution. Thus, the insect concentration should be considerable to produce a measurement in a limited time. This is particularly true if two-dimensional or three-dimensional mappings are desired.

With the experience gathered in the present work, it should be possible to perform lidar monitoring of insects of considerable impact on the ecology community.

References

1. R. M. Measures, *Laser Remote Sensing: Fundamentals and Applications* (Wiley, 1984).
2. S. Svanberg, "LIDAR," in *Springer Handbook of Lasers and Optics*, F. Träger, ed. (Springer, 2007), pp. 1031–1052.
3. X. Chu and G. C. Papen, "Resonance fluorescence lidar," in *Laser Remote Sensing* T. Fujii and T. Fukuchi, eds. (CRC, 2005), Chap. 5, pp. 179–432.
4. S. Svanberg, "Fluorescence spectroscopy and imaging of lidar targets," in *Laser Remote Sensing* T. Fujii and T. Fukuchi, eds. (CRC, 2005), Chap. 6, pp. 433–468,.
5. P. Weibring, H. Edner, and S. Svanberg, "Versatile mobile lidar system for environmental monitoring," Appl. Opt. **42**, 3583–3594 (2003).
6. L. Palombi, D. Lognoli, V. Raimondi, G. Cecchi, J. Hällström, K. Barup, C. Conti, R. Grönlund, A. Johansson, and S. Svanberg, "Hyperspectral fluorescence lidar imaging at the Colosseum, Rome: elucidating past conservation interventions," Opt. Express **16**, 6794–680 (2008).
7. M. Campero, F. Ollevier, and R. Stoks, "Ecological relevance and sensitivity depending on the exposure time for two biomarkers," Environ. Toxicol. **22**, 572–581 (2007).
8. R. Hickling, D. B. Roy, J. K. Hill, and C. D. Thomas, "A northward shift of range margins in British odonata," Glob. Change Biol. **11**, 502–506 (2005).
9. T. J. Case and M. L. Taper, "Interspecific competition, environmental gradients, gene flow, and the coevolution of species borders," Am. Nat. **155**, 583–605 (2000).
10. M. Joron and P. M. Brakefield, "Captivity masks inbreeding effects on male mating success in butterflies," Nature **424**, 191–194 (2003).
11. J. A. Shaw, N. L. Seldomridge, D. L. Dunkle, P. W. Nugent, L. H. Spangler, J. J. Bromenshank, C. B. Henderson, J. H. Churnside, and J. J. Wilson, "Polarization lidar measurements of honey bees in flight for locating land mines," Opt. Express **13**, 5853–5863 (2005).
12. K. S. Repasky, J. A. Shaw, R. Scheppele, C. Melton, J. L. Carsten, and L. H. Spangler, "Optical detection of honeybees by use of wing-beat modulation of scattered laser light for locating explosives and land mines," Appl. Opt. **45**, 1839–1843 (2006).
13. D. S. Hoffman, A. R. Nehrir, K. S. Repasky, J. A. Shaw, and J. L. Carlsten, "Range-resolved optical detection of honeybees by use of wing-beat modulation of scattered light for locating land mines," Appl. Opt. **46**, 3007–3012 (2007).
14. M. Brydegaard, Z. G. Guan, M. Wellenreuther, and S. Svanberg, "Insect monitoring with fluorescence lidar techniques: feasibility study," Appl. Opt. **48**, 5668–5677 (2009).
15. C. af Klinteberg, M. Andreasson, O. Sandström, S. Andersson-Engels, and S. Svanberg, "Compact medical fluorosensor for minimally invasive tissue characterization," Rev. Sci. Instrum. **76**, 034303 (2005).
16. P. S. Corbet, *Dragonflies: Behavior and Ecology of Odonata Essex* (Harley, 1999).
17. E. Anderson, Z. Bai, C. Bischof, S. Blackford, J. Demmel, J. Dongarra, J. Du Croz, A. Greenbaum, S. Hammarling, A. McKenney, and D. Sorensen, *LAPACK User's Guide*, 3rd ed. (Society for Industrial and Applied Mathematics, 1999).
18. R. Johansson, *System Modeling and Identification* (Prentice Hall, 1993).
19. E. M. C. Hillman and A. Moore, "All-optical anatomical co-registration for molecular imaging of small animals using dynamic contrast," Nat. Photon. **1**, 526–530 (2007).
20. R. B. Bradbury, R. A. Hill, D. C. Mason, S. A. Hinsley, J. D. Wilson, H. Balzter, G. Q. A. Anderson, M. J. Wittingham, I. J. Davenport, and P. E. Bellamy, "Modeling relationships between birds and vegetation structure using airborne lidar data: a review with case studies from agricultural and woodland environments," Ibis **147**, 443–452 (2005).
21. K. T. Vierling, L. A. Vierling, W. A. Gould, S. Martinuzzi, and R. M. Clawges, "Lidar: Shedding new light on habitat characterization and modeling," Front. Ecol. Environ. **6**, 90–98 (2008).
22. C. N. Parmesan, "Climate and species' range," Nature **382**, 765–766 (1996).
23. C. N. Parmesan, C. Ryrholm, C. Steganescu, J. K. Hill, C. D. Thomas, B. Descimon, B. Huntley, L. Kaila, J. Kullberg, T. Tammaru, W. J. Tennent, J. A. Thomas, and M. Warren, "Poleward shifts in geographical ranges of butterfly species associated with regional warming," Nature **399**, 579–583 (1999).
24. K. Tynkkynen, M. J. Rantala, and J. Suhonen, "Interspecific aggression and character displacement in the damselfly *Calopteryx splendens*," J. Evol. Biol. **17**, 759–767 (2004).

25. K. Tynkkynen, J. S. Kotiaho, M. Luojumäki, and J. Suhonen, "Interspecific aggression causes negative selection on sexual characters," Evolution **59**, 1838–1843 (2005).

26. K. Tynkkynen, J. S. Kotiaho, M. Luojumäki, and J. Suhonen, "Interspecific territoriality in *Calopteryx* damselflies: the role of secondary sexual characters," Anim. Behav. **71**, 299–306 (2006).

27. G. Rüppel, D. Hilfert-Rüppel, G. Rehfeldt, and C. Schütte, *Die Prachtlibellen Europas* (Westarp Wissenschaften, 2005).

28. A. Cordero, "Forced copulations and female contact guarding at a high male density in a *Calopterygid* damselfly," J. Insect Behav. **12**, 27–37 (1999).

29. A. Chaput-Bardy, A. Gregoire, M. Baguette, A. Pagano, and J. Secondi, "Condition and phenotype-dependent dispersal in a damselfly, *Calopteryx splendens*," PLoS ONE **5**, e10694 (2010).

30. K. F. Conrad, K. H. Willson, K. Whitfield, I. F. Harvey, C. J. Thomas, and T. N. Sherrat, "Characteristics of dispersing *Ischnura elegans* and *Coenagrion puella* (odonata): age, sex, size morph and ectoparasitism," Ecography **25**, 439–445 (2002).

31. L. Ward and P. J. Mill, "Habitat factors influencing the presence of adult *Calopteryx splendens* (odonata: Zygoptera)," Euro. J. Entomol. **102**, 47–51 (2005).

32. D. W. Gibbons and D. Pain, "The influence of river flow rate on the breeding behaviour of calopteryx damselflies," J. Anim. Ecol. **61**, 283–289 (1992).

33. F. S. Chapin, E. S. Zavaleta, V. T. Eviner, R. L. Naylor, P. M. Vitousek, H. L. Reynolds, D. U. Hooper, S. Lavore, O. E. SalaI, S. E. Hobbie, M. C. Mack, and S. Díaz, "Consequences of changing biodiversity," Nature **405**, 234–242 (2000).

34. P. M. Hammond, "Species inventory," in *Global Diversity Status of the Earth Living Resources*, B. Groombridge, ed. (Chapman and Hall, 1992), pp. 17–39.

35. J. A. Thomas, M. G. Telfer, D. B. Roy, C. D. Preston, J. J. D. Greenwood, J. Asher, R. Fox, R. T. Clarke, and J. H. Lawton, "Comparative losses of British butterflies, birds, and plants and the global extinction crisis," Science **303**, 1879–1881 (2004).